Indian Journal of Experimental Biology
Vol. 58, October 2020, pp. 680-690

Low dose of ^{131}I-F(ab')$_2$-Rituximab and ^{131}I-Rituximab induces G1arrest and apoptosis in Raji cells (Burkitt's lymphoma)

Shishu Kant Suman[1], Mythili Kameswaran[1]* & Ashutosh Dash[1,2]

[1]Radiopharmaceuticals Division, Bhabha Atomic Research Centre, Mumbai-400 085, Maharashtra, India
[2]Homi Bhabha National Institute, Anushakti Nagar, Mumbai-400 094, Maharashtra, India

Received 01 July 2019; *revised 22 June 2020*

Radiolabeled fragmented F(ab')$_2$ antibodies had shown better therapeutic efficacy than radiolabeled intact antibodies in treating cancers. In this study, we investigated the differences and similarities on the mechanism and extent of cell death in Raji cells (Burkitt's lymphoma) in response to 370 kBq of ^{131}I-F(ab')$_2$-Rituximab and ^{131}I-Rituximab up to 72 h. F(ab')$_2$ of Rituximab was prepared and characterized by SE-HPLC and SDS-PAGE. Fragmented and intact Rituximab were radioiodinated by Chloramine-T method. Toxicity and mechanism of cell death in Raji cells in response to ^{131}I-F(ab')$_2$-Rituximab and ^{131}I-Rituximab were studied by MTT (3-(4,5-dimethylthiazol-2-yl)-2,5-diphenyltetrazolium bromide), LDH (lactate dehydrogenase), trypan blue exclusion, viability, apoptotic, caspase assays and cell cycle analysis. The cytotoxicity assays showed slow death of Raji cells up to 24 h in response to both ^{131}I-F(ab')$_2$-Rituximab and ^{131}I-Rituximab. Cell cycle analysis at 30 h showed G1 arrest in Raji cells which led to its slow cell death up to 24 h. Elucidative assays to identify the molecular mechanism of death of G1arrested Raji cells showed apoptotic cell death at 40 h after treatment, which was validated by demonstrating caspase activation in arrested Raji cells. Toxicity studies and mechanism of cell death in Raji cells demonstrated comparable results when treated with equivalent doses (370 kBq) of radiolabeled antibodies indicating ^{131}I-F(ab')$_2$-Rituximab as a potential radioimmunotherapeutic agent for patients with Non-Hodgkin's lymphoma.

Keywords: Anticancer, Cell death, Cytotoxicity, Fragmented antibody, Radioiodination

Rituximab (MabThera, Rituxan) is a chimeric IgG1 monoclonal antibody that specifically targets the CD20 surface antigen expressed on normal and neoplastic B-lymphoid cells[1]. It is a FDA approved antibody that is widely used in the treatment of non-Hodgkin's Lymphoma [NHL][2]. NHL constitutes 4% of all cancers and ranks as the 6th most common cancer amongst females and the 7th most common cancer in males[3]. The incidence rate of NHL estimated in India was 22 per million (23,801 new cases) with a mortality rate of 15 per million (16,597 deaths) in 2012[4]. Rituximab radiolabeled with ^{131}I (^{131}I-Rituximab) is an useful radioimmunotherapeutic agent for NHL mainly due to its synergistic action of binding to specific tumor cells and β-radiations emitted by the ^{131}I, both of which facilitate in the killing of tumor cells[5]. Many clinical trials with ^{131}I-Rituximab in patients with NHL have shown a good overall response with some patients even attaining complete response[6-8]. The FDA approved radioimmunotherapeutic agent, ^{131}I-Tositumomab (Bexxar), that targets CD20 antigen has shown 70 % response rate in the treatment of patients with NHL[9,10]. Radioiodinated Rituximab has also been used in combination therapy or as an adjunct therapy for achieving better therapeutic ratio in patients with NHL[11,12]. However, the main disadvantages of using intact antibodies are their slow pharmacokinetics, poor tumor penetration, lower target to non-target ratio and risk of humoral effect due to the large size (~150 Kd) and the Fc region, all of which can be overcome by use of fragmented antibodies [F(ab')$_2$][13]. Reports indicate that radiolabeled F(ab')$_2$ promises to be a better theranostic agent as compared to intact antibody, when labeled with suitable theranostic radionuclides owing to its better pharmacokinetics, tumor penetration and high target to non-target ratio mainly due to its smaller size[14,15]. Various studies have reported that using radiolabeled F(ab')$_2$ as a theranostic agent yielded promising results[16,17]. As a result of the faster pharmacokinetics of F(ab')$_2$, ^{131}I-F(ab')$_2$ antibodies have exhibited better therapeutic effect than intact radiolabeled antibody in various tumor models and clinical trials[18-21].

*Correspondence
Phone: +91 09820300762
E-Mail: kmythili6@gmail.com,kmythili@barc.gov.in

Further, increased dose of $F(ab')_2$ fragments has shown to have enhanced therapeutic effect with no change in the minimal toxicity or normal tissue distribution pattern[18].The rapid clearance of $F(ab')_2$, allows delivery of twice the radiation dose to the tumor as compared to intact antibody, for the same blood dose in a colonic xenograft model[19].

In radioimmunotherapy (RIT), the radioimmuno-conjugates kill cancer cells predominantly by radioactive emissions from the radionuclides rather than due to the immunological effector functions[22]. The most commonly used radionuclides for RIT (I-131, Lu-177 and Y-90) kill tumor cells primarily by emission of beta (β-) particles, which are considered to induce DNA strand breaks[23]. I-131 is one of the radionuclide of choice for RIT largely due to its easy availability, suitable half-life (8 days), β-emission (606 keV; 90 %) of relatively short path length and ease of radiolabeling of biomolecules[24]. I-131 also emits γ rays of 364 keV, which permits simultaneous imaging of radiolabeled product enabling study of its pharmacokinetics and biodistribution *in vivo*[25].

Studies on cellular toxicity and its molecular mechanism in Raji cells in response to intact ^{131}I-Rituximab are scarce[5,26,27]. Here, in order to evaluate the potential of ^{131}I-$F(ab')_2$-Rituximab as a radio-immunotherapeutic agent for NHL, we carried out cytotoxicity studies, cellular arrest analysis, apoptosis and caspase assays in Raji cells in response to 370 kBq of both ^{131}I-$F(ab')_2$-Rituximab and ^{131}I-Rituximab.

Materials and Methods

Materials

Rituximab (MabThera, antiCD20 monoclonal antibody) was procured from Roche Inc., Basel, Switzerland. Iodine-131 was produced in-house by (n, γ) activation of tellurium oxide target and extracted by dry distillation technique. It was made available in the form of sodium iodide ($Na^{131}I$), pH 8-10[28]. All chemicals and reagents like MTT (3-(4,5-dimethyl-thiazol-2-yl)-2,5-diphenyltetrazolium bromide), sodium acetate, sodium chloride, sodium bicarbonate, HEPES, Roswell Park Memorial Institute medium (RPMI 1640) and trypan blue were procured from Sigma chemical Inc. (USA). Fetal Bovine Serum (FBS) was purchased from GIBCO Laboratories, USA. Assay kits for Cell cycle analysis, apoptosis, viability & caspase analyses were procured from Guava Technologies, Inc., Merck Millipore Corp., Germany. LDH assay kits were procured from Sigma chemical Inc. (USA). Immobilized Pepsin was obtained from Thermo Scientific while rProtein A Sepharose fast flow antibody affinity column and PD-10 columns were procured from GE Healthcare Life Sciences, USA. Protein molecular weight standards were procured from Bangalore Genei, India and /or GE Healthcare Ltd, UK and Amicon Ultra centrifugal filter devices (MW cut off 10 kDa and 50 kDa) were from Millipore, India. Well type NaI (Tl) detector (ECIL, India) was used for measuring radioactivity. Size exclusion HPLC (SE-HPLC) analysis were performed on a JASCO HPLC system (M/s. JASCO, Japan) coupled to a NaI (Tl) radio-activity detector (Raytest, Germany) and a PU 1575 UV/ visible detector (M/s. JASCO, Japan) using a TSK gel column (G3000 SWXL; 30 cm × 7.8 mm; 5 μm) from TOSOH Bioscience, USA. The chromatograms were assessed using the GINA STAR software (Version, M/s. Raytest GmBH, Germany). Guava EasyCyte Flow cytometer (Guava Technologies, Inc., Merck Millipore Corp. Germany) was used to acquire flow cytometry data and POLARstar Omega Plate Reader Spectrophotometer - BMG LABTECH, Germany was used to measure spectrometric reading. Raji cells (CD20 wildtype, Burkitt lymphoma cell line) were procured from National Centre for Cell Sciences, Pune, India.

Methods

Preparation, Purification and Characterization of $F(ab')_2$-Rituximab

Rituximab (MabThera, conc-10 mg/mL) was digested using bead immobilized pepsin in digestion buffer (20 mM sodium acetate solution, pH-4.5) at 37°C for 18 h with continuous high speed shaking. The crude digest was purified using Amicon Ultra centrifugal filter devices (MW cut off 50000Da) and rProtein A Sepharose fast flow column sequentially. Flow through from Sepharose-rProtein A column was collected as 2 mL fractions which contained the purified $F(ab')_2$ fragments. The $F(ab')_2$ fragments were characterized by gradient SDS-PAGE (5-15 %) under both reducing and non-reducing conditions[29].

Radioiodination and Characterization of $F(ab')_2$-Rituximab & Rituximab

Fragmented Rituximab ($F(ab')_2$-Rituximab) and intact Rituximab were radioiodinated using the Chloramine-T method[30]. Briefly, to the reaction vial containing 200 μL of 0.5 M phosphate buffer, pH 7.6, $F(ab')_2$-Rituximab (400 μg) or Rituximab (500 μg) and 1.5 mCi (55.5 MBq) of I-131 activity was added. This was followed by addition of 15 µL (~30 µg) of freshly prepared Chloramine-T in 0.05 M phosphate buffer, pH 7.4. After 90 s of reaction time, 45 µL (90 µg) of sodium metabisulphite in 0.05 M phosphate buffer, pH 7.4 was added, gently mixed and incubated for 60 s. The reaction was finally terminated with 100 µL (100 µg) of KI. The radiolabeled $F(ab')_2$-Rituximab and Rituximab were purified by passing each through PD-10 desalting columns using 0.05 M phosphate buffer, pH 7.4 for elution. Labeling efficiency and specific activity were calculated. The radiochemical purity (RCP) of ^{131}I-$F(ab')_2$-Rituximab and ^{131}I-Rituximab was determined by SE-HPLC using a TSK gel column wherein elution was carried out isocratically with 0.05 M phosphate buffer containing 0.05% sodium azide (pH 6.8) at a flow rate of 0.6 mL/min.

In vitro cell Binding and Inhibition studies

Cell binding and inhibition studies with ^{131}I-$F(ab')_2$-Rituximab and ^{131}I- Rituximab were carried out in Raji cells that express CD20 on their cell surface. Cells were grown to 60-70% confluence in RPMI medium containing 10% FBS in a humidified CO_2 incubator at 37ºC. Cells were then harvested and 1×10^6 cells/well was layered in 12 well tissue culture plates. For cell binding studies, 1µg/mL of ^{131}I-$F(ab')_2$-Rituximab and/or 1µg/mL of ^{131}I-Rituximab were added and incubated for 2 h at 37ºC. All studies were carried out in triplicates. After incubation, the cells were washed twice with 1.0 mL of 0.05 M phosphate buffer saline (PBS) (pH 7.4) and centrifuged at 2000 rpm for 20 min at room temperature (RT) of 25°C. The supernatant was aspirated and the cell pellet measured for radioactivity.

For inhibition studies, unlabeled Rituximab (10 µg and 50 µg) was co-incubated with 1 µg/mL of ^{131}I-$F(ab')_2$-Rituximab and/or ^{131}I-Rituximab. The assays were carried out under identical conditions as mentioned earlier. The percentage cell binding and inhibition were calculated to determine the specificity of ^{131}I-$F(ab')_2$-Rituximab and ^{131}I-Rituximab to CD20 antigen.

Cytotoxicity studies

In case of assays for cytotoxicity (MTT, LDH, trypan blue exclusion and viability assays), Raji cells were cultured in RPMI medium containing 10% FBS and grown up to 60-70% confluence. After harvesting, 1×10^6 cells were seeded in 12 well tissue culture plates and treated with 370 kBq (~35.8 µGy) of ^{131}I-$F(ab')_2$-Rituximab and/or ^{131}I-Rituximab and incubated for various time intervals depending on the assay to be carried out. Concurrently, another set of cells were treated with equivalent amount of unlabeled $F(ab')_2$-Rituximab (2.7 µg) and Rituximab (3.3 µg) as unlabeled vehicle controls for ^{131}I-$F(ab')_2$-Rituximab and ^{131}I-Rituximab, respectively. Control set of cells were left untreated. All treatments were carried out in triplicates.

MTT assay

MTT (3-(4, 5-dimethylthiazol-2-yl)-2, 5-diphenyltetrazolium bromide) assay which is a colorimetric assay was used to measure cellular metabolic activity and hence the cell viability. Viable cells that contain NAD(P)H-dependent oxidoreductase enzymes reduce the MTT reagent to formazan, to give a deep purple colour[31]. Herein, 50 µL (~0.5×10^5 Raji cells) of each cell sample harvested in serum free media, treated with ^{131}I-$F(ab')_2$-Rituximab, ^{131}I-Rituximab, unlabeled $F(ab')_2$-Rituximab and unlabeled Rituximab, was mixed with 50 µL of MTT solution (5 mg/mL in PBS) and incubated at 37°C for 3 h. After incubation, 150 µL of MTT solvent (4 mM HCl, 0.1% NP40 in isopropanol) was added and incubated for 15 min under shaking condition for dissolution of formazan. Reaction was stopped by adding 1/10 volume of 1N HCl and absorbance read at 590 nm. The % of dead cells was calculated as ([optical density (OD) of control sample - OD of treated sample/OD of control sample]*100). This was plotted against the different time points (8, 16, 24, 48 and 72 h) after treatment with the labeled and unlabeled antibodies [viz. ^{131}I-$F(ab')_2$-Rituximab, ^{131}I-Rituximab, unlabeled $F(ab')_2$-Rituximab and Rituximab]

LDH assay

Lactate Dehydrogenase (LDH) assay is a colorimetric assay to quantitatively measure LDH released into the media from damaged cells as a biomarker for cellular cytotoxicity and hence, a direct measure of the cell death. The procedure was carried out as per the reported protocol[27]. Herein, 100 µL of Raji cells (~1×10^5 cells) each treated with ^{131}I-$F(ab')_2$-Rituximab, ^{131}I-Rituximab, unlabeled $F(ab')_2$-Rituximab and unlabeled Rituximab were centrifuged at 8, 24, 48 and 72 h post treatment and the supernatant was collected. This supernatant was mixed with LDH assay mixture (2:1, v/v) in 96 well plates and incubated at RT for 25 min in dark. LDH assay mixture was made by mixing the dye with equal volumes of substrate and cofactor of LDH just before use. After incubation, the reaction was stopped by addition of 1/10 volume of 1 N HCl and the absorbance measured at 490 nm. The % of dead cells represented as % release of LDH was calculated and plotted against different time points post treatment with the antibodies.

Trypan Blue exclusion viability assay

Additional viability assay i.e. trypan blue exclusion assay was carried out wherein the intact cells appear transparent while the dead cells take up the trypan blue dye and appear blue when viewed under the microscope. For this assay, 10 µL of 0.4% Trypan blue solution was mixed with 10 µL of the Raji cells (~1×10^4 cells) treated with ^{131}I-F(ab')$_2$-Rituximab, ^{131}I-Rituximab, unlabeled F(ab')$_2$-Rituximab and Rituximab. The samples were counted for viability using a hemocytometer at 6, 16, 24, 48, and 72 h post treatment. The % dead cells was calculated and plotted as compared to the control cells at different time points post treatment.

Viability assay

Viability count assay was performed as per the procedure specified in the Guava ViaCount assay kit, Guava Technologies, Millipore. 50 µL of cell sample (~0.5×10^5 cells) each treated with ^{131}I-F(ab')$_2$-Rituximab, ^{131}I-Rituximab, unlabeled F(ab')$_2$-Rituximab and Rituximab were mixed with 450 µL of Guava ViaCount reagent and incubated for 5 min at RT in dark. The viable count assay distinguishes the viable and non-viable cells based on the differential permeability's of the two DNA-binding dyes. The nuclear dye stains only nucleated cells while the viability dye stains only the dead cells. Sample acquisition and data analysis were performed using the ViaCount software module in Guava EasyCyte Flow cytometer. The % dead cells as compared to control samples were calculated and plotted in response to the different treatments given at 24 and 48 h post treatment.

Cell cycle analysis

Cell cycle analysis is based on the amounts of DNA present at different stages of the cell cycle, which is detected by the DNA-binding dye fixed on cells and acquired on a flow cytometer. In order to investigate the slow death up to 24 h, cell cycle analysis was performed at 30 h after treatment of Raji cells with^{131}I-F(ab')$_2$-Rituximab, ^{131}I-Rituximab, unlabeled F(ab')$_2$-Rituximab and Rituximab. Raji cells were processed as per the procedure given in Guava cell cycle kit. Briefly, the cells (~1×10^6 cells) were washed with PBS (0.05 M, pH 7.4) and fixed in 70% ice-cold ethanol. The cells were kept at 4ºC for 1 h prior for staining. Herein, ethanol was completely removed from the cell suspension by repeated washes with 0.05 M PBS, pH 7.4, resuspended in 200 µL Guava cell cycle reagent and incubated for 30 min at RT in dark. Sample data were acquired using the Cell Cycle software module in Guava EasyCyte Flow cytometer and analyzed using Cyflogic software. The percentage of cells acquired from the treated groups as compared to the control at different stages of cell cycle were analyzed and plotted for the different treatments given.

Apoptotic assay

Apoptotic assay was performed to determine the mode of death of the arrested Raji cells. The cell samples treated with ^{131}I-F(ab')$_2$-Rituximab, ^{131}I-Rituximab, unlabeled F(ab')$_2$-Rituximab and rituximab were processed at 40 h post treatment as per the protocol specified in the Guava Apoptotic kit. Briefly, 100 µL of treated cell samples were mixed with 100 µL of Guava annexin reagent and incubated for 20 min at RT in dark. Nexin reagent contains annexin V-PE that binds to phosphatidyl serine (PS) which is an indicator of apoptosis. Nexin reagent also contains a cell impermeant DNA binding dye 7-AAD (7-aminoactinomycin D) which determines the membrane integrity. Sample acquisition and data analysis were performed using the Nexin software module in Guava EasyCyte Flow cytometer. The % of cells in early to mid stages of apoptosis were compared to control cells and plotted for the different treatments given.

Caspase assay

Caspase assay was carried out to check the caspase activation for validation of apoptotic death of arrested Raji cells in G1 stage. Activation of Capase 3 and 7 was determined using the Guava Easy Cyte caspase 3/7 kit. This kit uses a FLICA (Fluorescent labeled inhibitor of Caspases) consisting of 3 subunits - an amino acid inhibitor sequence recognized by caspase 3/7 aspartic acid-glutamic acid-valine-aspartic acid (DEVD), a fluoromethyl ketone moiety which covalently binds active caspase 3/7 enzymes and a carboxyfluorescein (FAM) reporter. Unbound FLICA diffuses out of cell while FLICA positive cells (Caspase +) correspond to apoptotic cells. The cell impermeant DNA binding dye 7-AAD (7-amino-actinomycin D) permits simultaneous evaluation of caspase activity and membrane integrity.

The ^{131}I-F(ab')$_2$-Rituximab, ^{131}I-Rituximab, unlabeled F(ab')$_2$-Rituximab and Rituximab treated cell samples were processed as per the procedure given in the Guava caspase kit, Guava Technologies, Millipore. Briefly, 100 µL of treated cell samples (~1×10^5 cells) were mixed with 10 µL of caspase reagent solution and incubated for 1 h at 37°C in a CO_2 incubator. The cells were washed twice with 1X apoptosis wash buffer and incubated with 200 µL of caspase 7-AAD working solution for 10 min at RT. Sample acquisition and data analysis were carried out using the Caspase software module in Guava EasyCyte Flow cytometer. The % of treated cells showing caspase activation as compared to control samples were analyzed at 40 h post treatment and plotted for the different treatments given.

Statistical analysis

All experiments are performed in triplicates. Results given are mean ± standard error of at least 3 independent experiments. All statistical analyses were performed using the one-way analysis of variance (ANOVA) followed by Post-hoc Bonferroni test to compare between different pair of treatments for determining the significance value**.** $P \leq 0.05$ was considered statistically significant.

Results

Preparation, purification and characterization of $(Fab')_2$ of Rituximab

Standardization experiments revealed that in order to achieve maximum digestion, the optimum time for digestion of Rituximab with pepsin was 18 h. From 10 mg of Rituximab originally taken for digestion, 7.86 mg $F(ab')_2$-Rituximab (78.6%) was obtained. Purified $F(ab')_2$-Rituximab was characterized by SDS-PAGE under non-reducing and reducing conditions. Under non-reducing conditions, the purified $F(ab')_2$-Rituximab exhibited a molecular weight of ~100 kDa by SDS-PAGE (Fig. 1A), while under reducing conditions, the heavy and light chain bands were observed at ~29 and ~25 kDa, respectively (Fig. 1B).

Radioiodination of $F(ab')_2$ of Rituximab/Intact Rituximab and their characterization

The labeling efficiency of radioiodination of $F(ab')_2$-Rituximab and Rituximab was 92-93 % while the specific activity was determined to be 136.9 kBq/µg for $F(ab')_2$-Rituximab and 111 kBq/µg for Rituximab. SE-HPLC chromatograms of ^{131}I-$F(ab')_2$-Rituximab and ^{131}I-Rituximab showed a single peak with retention times of 15.34 min and 14.51 min, respectively which corresponded to the unlabeled counterparts (Fig. 2 A and B).

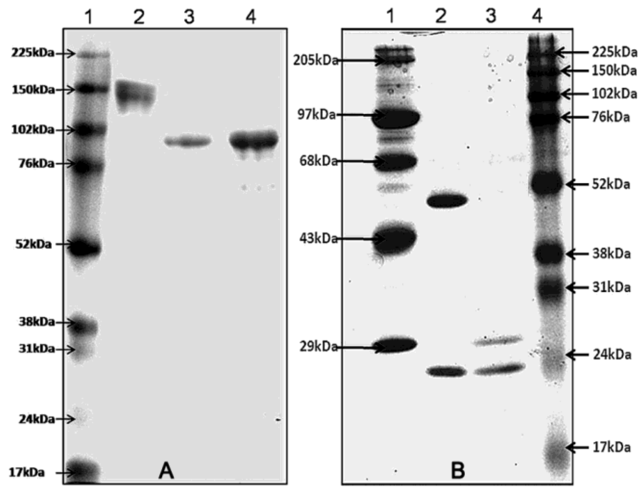

Fig. 1 — SDS-PAGE on 5-15% gradient gel. (A) Under non-reducing conditions - (Lane 1: Protein molecular weight standards, Lane 2: Intact Rituximab (15 µg), Lane 3: $F(ab')_2$ of Rituximab (20µg), Lane 4: $F(ab')_2$ of Rituximab (40µg); (B) Under reducing conditions using β-mercaptoethanol - (Lane1: Protein molecular weight standards (GE Healthcare), Lane 2: Intact Rituximb (15 µg), Lane 3: $F(ab')_2$ of Rituximab (20 µg), Lane 4: Protein molecular standard (Bangalore Genei)

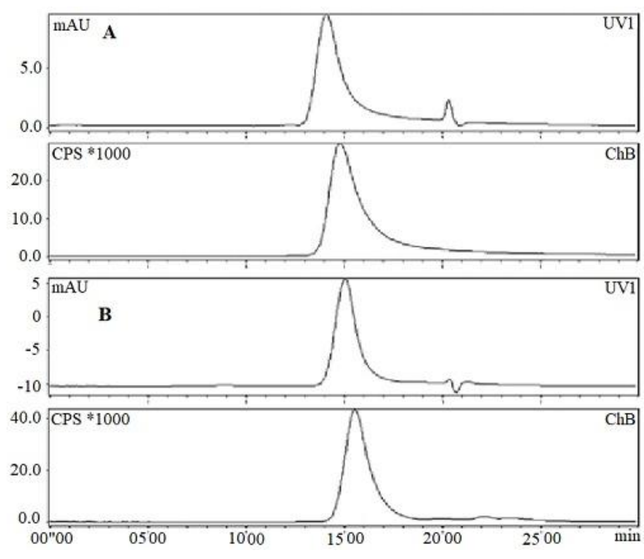

Fig. 2 — Size exclusion HPLC chromatogram of (A) ^{131}I-Rituximab; and (B) ^{131}I-$F(ab')_2$-Rituximab on a TSK gel column by isocratic elution with 0.05 M phosphate buffer + 0.05% sodium azide (pH 6.8) at 0.6 mL/min. [RCP of radioimmunoconjugates > 95%; (R_t of ^{131}I-Rituximab=14.51 min; R_t of ^{131}I-$F(ab')_2$-Rituximab =15.34 min)]

Cell binding and inhibition studies

Cell binding and inhibition studies were carried out with ^{131}I-$F(ab')_2$-Rituximab and ^{131}I-Rituximab in Raji cells to determine their specificity to the CD20 antigens after radioiodination. As indicated in Fig. 3,

^{131}I-F(ab')$_2$-Rituximab showed a binding of 12.9±1.3% which was comparable to the binding exhibited by ^{131}I-Rituximab of 12.2±0.6%; ($P \leq 0.05$). Similarly, inhibition studies with 10 µg and 50 µg of unlabeled Rituximab showed comparable results for both ^{131}I-F(ab')$_2$-Rituximab and ^{131}I-Rituximab indicating that the specificity of F(ab')$_2$-Rituximab or intact Rituximab to the CD20 antigen was retained after radioiodination. Inhibitions of 21.7% and 26.4 % were observed when ^{131}I-F(ab')$_2$-Rituximab was co-incubated with 10 µg and 50 µg of unlabeled Rituximab, respectively while the inhibitions were 14 and 18% when ^{131}I-Rituximab was co-incubated with 10 µg and 50 µg of unlabeled Rituximab, respectively (Fig. 3).

Cytotoxicity studies

The extent of death of Raji cells in response to 370 kBq of ^{131}I-F(ab')$_2$-Rituximab and ^{131}I- Rituximab was determined to be similar (P <0.05) by the different cytotoxicity assays performed. A 2-3 fold higher cytotoxicity was observed when the cells were treated with ^{131}I-F(ab')$_2$-Rituximab and /or ^{131}I- Rituximab as compared to their unlabeled vehicle controls.

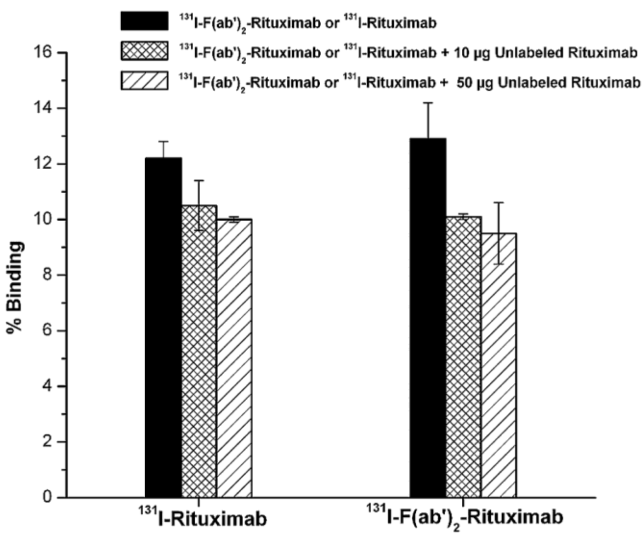

Fig. 3 — Cell binding studies with ^{131}I-Rituximab & ^{131}I-F(ab')$_2$-Rituximab in Raji cells. Inhibition studies with 10 and 50 µg of unlabeled Rituximab

MTT assay

MTT assay directly correlates with the cell viability. The % cell death of Raji cells treated with ^{131}I-F(ab')$_2$-Rituximab, ^{131}I-Rituximab, unlabeled F(ab')$_2$-Rituximab and Rituximab were compared with the untreated control cells at different time points up to 72 h. The % cell death compared to untreated control was plotted against the different time points studied post treatment as indicated in Fig. 4A. It is evident that the cytotoxicity in Raji cells in response to ^{131}I-F(ab')$_2$-Rituximab and ^{131}I-Rituximab were comparable and not statistically different (P <0.05). Moreover, the % cell death was 2-3 fold higher in those Raji cells treated with ^{131}I-F(ab')$_2$-Rituximab and ^{131}I-Rituximab as compared to cells treated with unlabeled vehicle control F(ab')$_2$-Rituximab and Rituximab.

LDH Assay

LDH released from damaged cell is a direct measure of cytotoxicity. The % cell death of Raji cells post treatment with ^{131}I-F(ab')$_2$-Rituximab, ^{131}I-Rituximab, unlabeled F(ab')$_2$ and Rituximab were compared with the untreated control Raji cells and plotted against the time points post treatment. As shown in Fig. 4B, death of Raji cells in response to ^{131}I-F(ab')$_2$-Rituximab and ^{131}I-Rituximab was 12.9±1.08 and 15.4±0.4%, respectively at 8 h. which increased to 97.3±1.3 and 95.3±1.02% at 72 h, respectively. The % cell death of Raji cells in response to ^{131}I-F(ab')$_2$-Rituximab and ^{131}I- Rituximab was determined to be comparable ($P \leq 0.05$) and more than 2-3 fold as compared to unlabeled F(ab')$_2$-Rituximab and Rituximab, respectively.

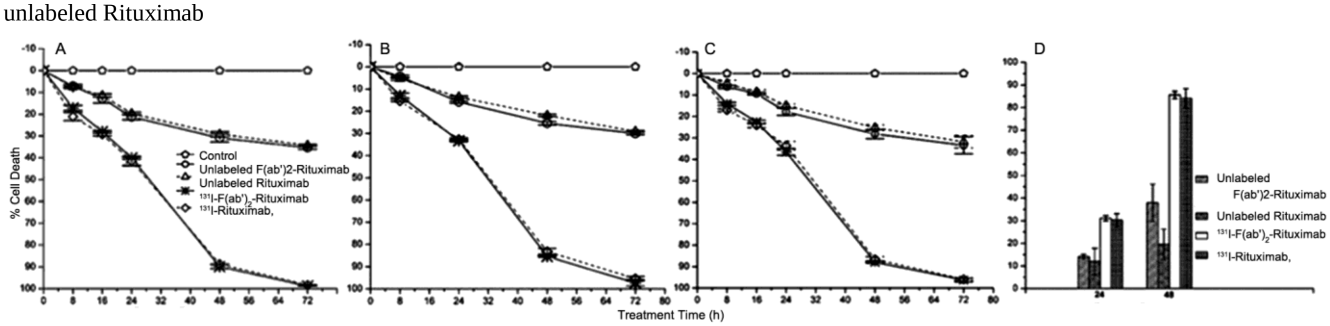

Fig. 4 — Scatter plot of the cytotoxicity assays - (A) MTT assay; (B) LDH assay; (C) Trypan Blue exclusion viability assay; and (D) histogram plot of viability assay showing % cell death in response to ^{131}I-F(ab')$_2$-Rituximab, ^{131}I-Rituximab, unlabeled F(ab')$_2$-Rituximab and Rituximab as compared to untreated control cells at different time points post treatment

Trypan Blue exclusion viability assay

In the Trypan blue assay, the transparent viable cells and blue stained non-viable cells were counted. The % dead cells post treatment with ^{131}I-F(ab')$_2$-Rituximab, ^{131}I-Rituximab, unlabeled F(ab')$_2$-Rituimab and Rituximab compared to untreated control cells were plotted against different time points post treatment (Fig. 4C). Here again, a comparable degree of cell death of Raji cells was observed in response to ^{131}I-F(ab')$_2$-Rituximab and ^{131}I-Rituximab ($P \leq 0.05$) which was 2-3 fold higher when treated with unlabeled F(ab')$_2$-Rituximab and Rituximab at different time points.

Viability assay

Viability assay measures the % viability of cells treated with ^{131}I-F(ab')$_2$-Rituximab, ^{131}I-Rituximab, unlabeled F(ab')$_2$-Rituximab and Rituximab in the sample. The % cell death of treated Raji cells as compare to untreated control cells at 24 h and 48 h post treatment were calculated and plotted as indicated in Figure 4d. It is evident that the extent of cytotoxicity exhibited by both ^{131}I-F(ab')$_2$-Rituximab and ^{131}I-Rituximab are similar ($P \leq 0.05$) and 2-3 fold higher than that exhibited by their unlabeled counterparts at 24 and 48 h.

Cell cycle analysis

To investigate the comparatively slow death of Raji cells up to 24 h, cell cycle analysis of treated Raji cells was carried out at 30 h. Fig. 5 (A-E) represents the cell cycle data as analyzed by Cyflogic software. The % of cells at different stages of cell cycle was compared between the different treatments given, which indicated that Raji cells were arrested in G1 stage of the cell cycle. The % of cells in the G1 stage were calculated and plotted as compared to untreated control cells in response to different treatments. Fig. 5F is the graphical representation of the % of cells which are in G1 stage as compared to untreated control cells. This was determined to be 7.4±0.6 and 9.9±2.0% in response to F(ab')$_2$-Rituximab and Rituximab, respectively while it was 35.6±7.2 and 39.8±8.5% in response to ^{131}I-F(ab')$_2$-Rituximab and ^{131}I-Rituximab, respectively. These results are comparable with each other ($P < 0.05$).

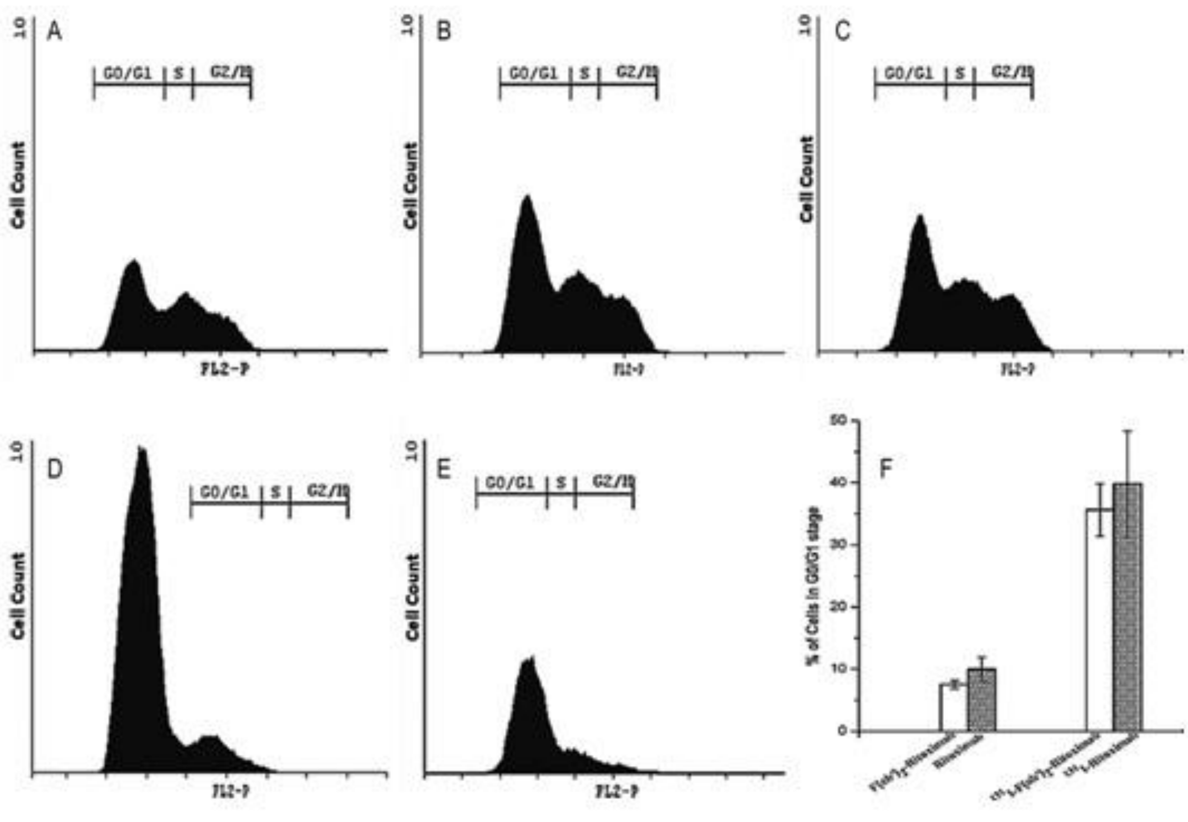

Fig. 5 — Flow cytometry cell cycle analysis: (A) untreated control Raji cells. Cell cycle progress in Raji cells in response to treatment with (B) unlabeled Rituximab; (C) unlabeled F(ab')$_2$-Rituximab; (D) ^{131}I-Rituximab; (E) ^{131}I-F(ab')$_2$-Rituximab; and (F) Histogram representation of the number of Raji cells in G0/G1stage compared to untreated control cells. [This plot was obtained from the data of (A) to (E) undoubtedly indicating G0/G1 arrest of Raji cells in response to the various treatments given]

Apoptosis assay

To determine the mode of death of the arrested Raji cells, apoptosis assay was performed at 40 h. Fig. 6 (A-E) represents the apoptotic data acquired by Nexin software module in Guava EasyCyte Flow cytometer. Lower-right side quadrant of the double plot represents % of cells in early to mid stage of apoptosis. Fig. 6F is the graphical representation of the % of cells undergoing apoptotic death as compared to untreated control cells. This was calculated and plotted in response to different treatments given. It was observed that the % of cells in early to mid stage of apoptosis compared to untreated control in response to ^{131}I-F(ab')$_2$-Rituximab and ^{131}I-Rituximab was 372.5±12.7 and 357.6±12.3%, respectively. Apoptosis induced in response to 370 kBq of ^{131}I-F(ab')$_2$-Rituximab and ^{131}I-Rituximab were comparable and not significantly different ($P \leq 0.05$). These results indicated that one of the modes of the death in arrested Raji cells in G1 stage were by apoptosis.

Caspase assay

Apoptotic death was validated by demonstrating caspase 3 and 7 activation using caspase assay in the arrested Raji cells at 40 h. Fig. 7 (A-E) illustrates the typical data of caspase activation acquired in by Caspase software in Guava EasyCyte Flow cytometer. Lower and upper right side quadrants of the double plot depict the cells having active caspase activity. The % of cells showing caspase activation as compared to untreated control cells were calculated and plotted in response to different treatments given (Fig.. 7F). The results showed that 181.6±0.1 and 161.8±2.3% of the cells have caspase activation (caspase +) as compared to untreated control cells in response to ^{131}I-F(ab')$_2$-Rituximab and ^{131}I- Rituximab, respectively. On the other hand, the % of cells that have caspase activation (caspase +) as compared to untreated

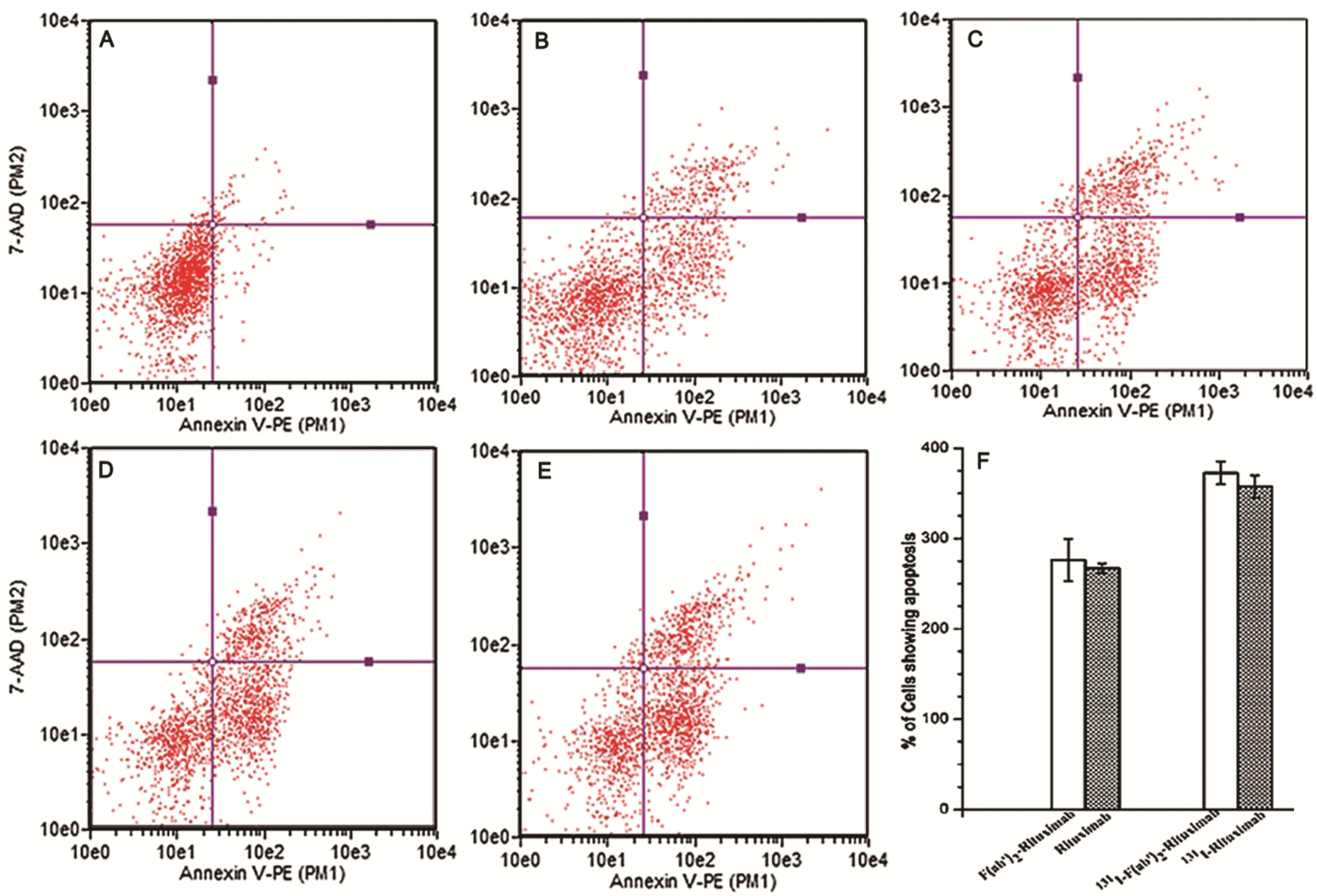

Fig. 6 — Flow cytometry analysis of annexin-V and 7-AAD (7-Aminoactinomycin D) staining of apoptotic cells of Raji cells. (A) untreated control Raji cells. Raji cells in response to treatment with (B) unlabeled Rituximab; (C) unlabeled F(ab')$_2$-Rituximab; (D) ^{131}I-Rituximab; (E) ^{131}I-F(ab')$_2$-Rituximab; and (F) Histogram representation of the % of apoptotic cells compared to untreated control cells in response to the different treatments given

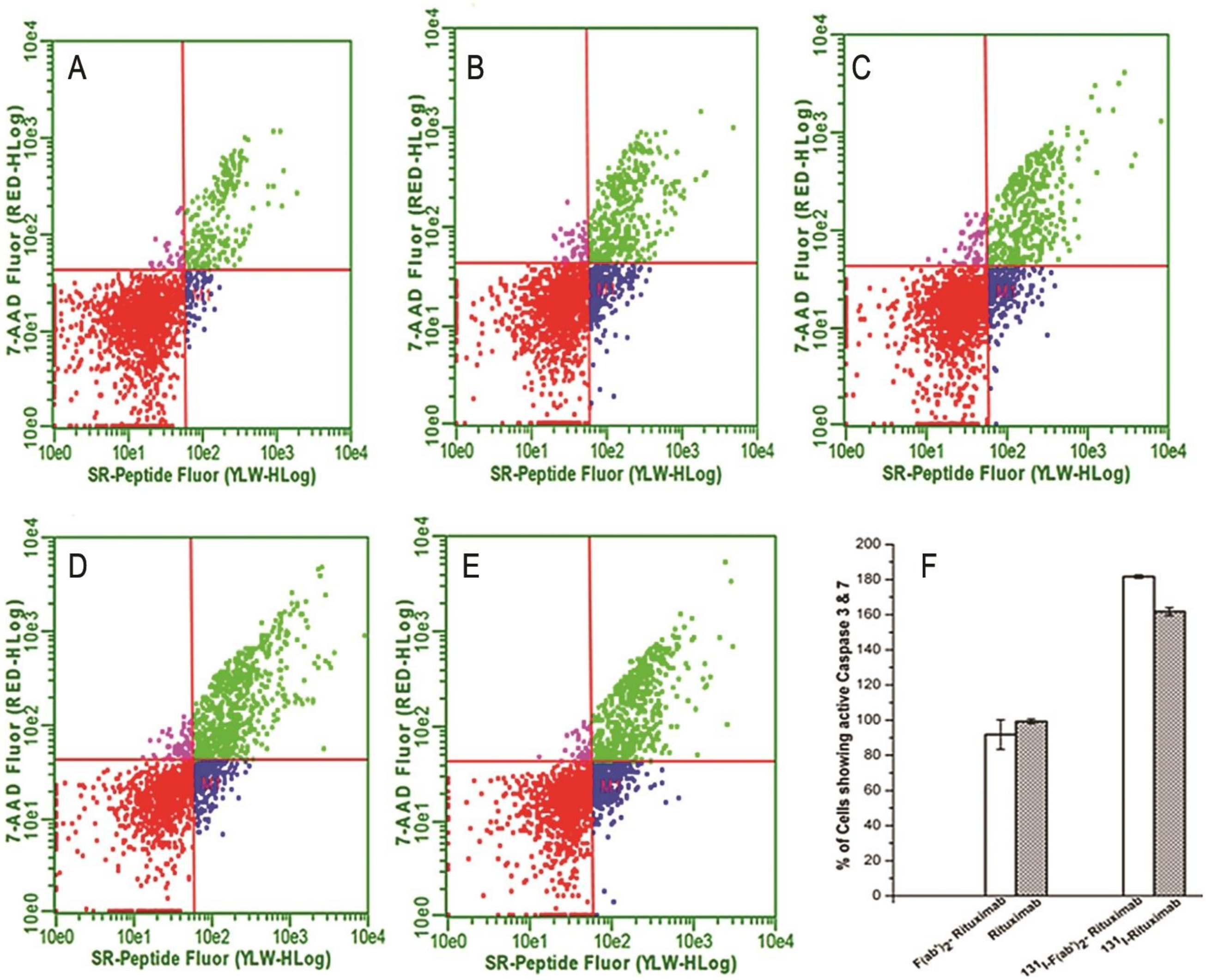

Fig. 7 — Flow cytometry analysis (A-E) for caspase 3 and 7 activation to validate apoptotic death in Raji cells at 40 h post treatment. (A) untreated control Raji cells. Raji cells in response to treatment with (B) unlabeled Rituximab; (C) unlabeled $F(ab')_2$-Rituximab; (D) ^{131}I-Rituximab; (E) ^{131}I-$F(ab')_2$-Rituximab; and (F) demonstrates caspase 3 and 7 activation in Raji cells compared to untreated control cells at 40 h in response to the different treatments given

control cells in response to unlabeled $F(ab')_2$-Rituximab and unlabeled Rituximab was 91.8±8.4 and 99.3±0.6%, respectively.

Discussion

Longer circulation time, non-specific binding and formation of immune responses have limited the utilization of monoclonal antibody in clinical oncology. $F(ab')_2$ of antibody has added advantages of faster pharmacokinetics, rapid clearance from body, high tumor / blood ratio, favorable imaging kinetics, better tumor penetration, lower immunogenicity potential and low non-specific binding largely due to its smaller size and absence of the Fc region as compared to the intact antibody[13]. Another therapeutic advantage of $F(ab')_2$ over intact monoclonal antibody is its minimal toxicity to organs due to its rapid clearance, thereby permitting administration of multiple doses and demonstration of high tumor/non-tumor uptake after treatment[18,32]. Hence, $F(ab')_2$ of antibody are more preferred for radioimmunotherapy and radioimmunoscintigraphy. $F(ab')_2$ has been used for improved radioimaging, tumor localization and scintigraphy of colorectal carcimoma[33,34]. Clinical trials using $F(ab')_2$-antibodies for radioimmunotherapy of metastatic colorectal cancer, gastrointestinal cancer and patients with glioblastomas have also been successfully carried out[14,35].

The present study was aimed at studying the cytotoxicity and mechanism of cell death in Raji cells in response to ^{131}I-F(ab')$_2$-Rituximab. This would provide insight of the feasibility of using ^{131}I-F(ab')$_2$-Rituximab as a radioimmunodiagnostic and radio-immunotherapeutic agent for NHL. Hence, a comparative study on the cytotoxicity and molecular mechanism of cell death in Raji cells was carried out to determine the similarities and differences in response to ^{131}I-F(ab')$_2$-Rituximab and ^{131}I-Rituximab. Cytotoxicity investigation in Raji cells treated with ^{131}I-F(ab')$_2$-Rituximab and ^{131}I-Rituximab showed comparable extent of toxicity at different time points studied i.e. 8, 16, 24, 48 , and 72 h post treatment. There was an overall 2-3 fold higher cytotoxicity with ^{131}I-F(ab')$_2$-Rituximab and ^{131}I-Rituximab in Raji cells as compared to Raji cells treated with unlabeled F(ab')$_2$-Rituximab and Rituximab. Reports revealed similar results wherein Raji cells treated with ^{131}I-Rituximab (1.85 MBq for 2 h) had significantly higher toxicity (~2-2.5 fold higher) at 24 h as compared to cells treated with the same concentration of unlabeled Rituximab[27]. Raji cells treated with ^{131}I-Rituximab for 2 h with 1.85 MBq exhibited ~22% cell death at 8 hour as compared to ~15% cell death by unlabeled rituximab[5]. ^{131}I-Rituximab showed significantly higher growth inhibition rate of the cells as compared to unlabeled Rituximab ($P \leq 0.05$) at a specific activity of 60 µCi/mL[26]. The comparable degree of similarity exhibited by ^{131}I-F(ab')$_2$-Rituximab with ^{131}I-Rituximab favours the use of ^{131}I-F(ab')$_2$-Rituximab as an effective radioimmuno-conjugate with its added attributes, for both diagnosis and treatment of NHL.

In this study, Raji cells showed G1 arrest at 30 h and apoptotic mode of death at 40 h in response to both ^{131}I-F(ab')$_2$-Rituximab and ^{131}I-Rituximab. Similar studies showed that majority of the Raji cells were arrested at G(1)/G(2) stage when treated with ^{131}I-Rituximab[36]. The apoptotic rate in these Raji cells were 51.99% in ^{131}I-Rituximab group, 29.42% in Rituximab group and 26.17% in the untreated control group[36]. In an another study, Raji cells when treated with ^{131}I-Rituximab (1.85 MBq for 2 h) showed ~2.5 fold at 2-8 h and ~25 fold at 24 h higher apoptosis as compared to untreated control Raji cells[5,27]. On the other hand, Raji cells treated with unlabeled Rituximab showed ~2.5 fold at 2 h and ~4 fold at 24 h higher apoptosis, as compared to untreated control cells[5,27]. These observations suggest that both ^{131}I-F(ab')$_2$-Rituximab and ^{131}I-Rituximab may have similar cytotoxicity *in vivo* as well. Further, animal studies are essential to study the cytotoxicity of ^{131}I-F(ab')$_2$-Rituximab *in vivo,* its degree of tumor penetration and target to non-target ratio as compared to ^{131}I-Rituximab to confirm its utility as a good radioimmunotherapeutic agent for NHL.

Conclusion

Results of this study advocate the use of fragmented antibody (^{131}I-F(ab')$_2$-Rituximab) as a radioimmunotherapeutic agent as it has shown comparable degree of cytotoxicity and similar mechanism of cell death *in vitro* in Raji cells when compared with intact Rituximab (^{131}I-Rituximab). This study would help in realizing the potential of ^{131}I-F(ab')$_2$-Rituximab as an efficient radioimmuno-therapeutic agent for NHL. However, biodistribution and pharmacokinetic studies of ^{131}I-F(ab')$_2$-Rituximab in tumor model studies are warranted to confirm the same *in vivo.*

Acknowledgement

Research at the Bhabha Atomic Research Centre is fully funded by the Government of India. The authors are grateful to Dr PK Pujari, Associate Director, Radiochemistry and Isotope Group for supporting this project. Authors gratefully acknowledge staff of Radiochemicals Section, RPhD, BARC for supply of ^{131}I activity.

Conflict of Interest

Authors declare no conflict of interests.

References

1 Pierpont TM, Limper CB &. Richards KL, Past, Present, and Future of Rituximab—The world’s First Oncology Monoclonal Antibody Therapy. *Front Oncol*, 8 (2018) 163.

2 Jayashree BS, Nigam S, Pai A, Patel HK, Reddy ND, Kumar N & Rao CM, Targets in anticancer research—A review. *Indian J Exp Biol*, 53 (2015) 489.

3 Chihara D, Nastoupil LJ, Williams JN, Lee P, Koff JL & Flowers CR. New insights into the epidemiology of non-Hodgkin lymphoma and implications for therapy. *Expert Rev Anticancer Ther*, 15 (2015) 531.

4 Danduga RC, Kola PK & Matli B, Anticancer activity of curcumin alone and in combination with piperine in Dalton lymphoma ascites bearing mice. *Indian J Exp Biol*, 58 (2020) 181.

5 Kumar C, Pandey BN, Samuel G & Venkatesh M, Doxorubicin enhances ^{131}I-rituximab induced cell death in Raji cells. *J Cancer Res Ther*, 11 (2015) 823.

6 Bienert M, Reisinger I, Srock S, Humplik BI, Reim C, Kroessin T, Avril N, Pezzutto A & Munz DL, Radio-immunotherapy using 131I-rituximab in patients with

advanced stage B-cell non-Hodgkin's lymphoma: initial experience. *Eur J Nucl Med Mol Imaging*, 32 (2005) 1225.

7 Leahy MF, Seymour JF, Hicks RJ & Turner JH, Multicenter phase II clinical study of iodine-131-rituximab radioimmunotherapy in relapsed or refractory indolent non-Hodgkin's lymphoma. *J Clin Oncol*, 24 (2006) 4418.

8 Leahy MF & Turner JH, Radioimmunotherapy of relapsed indolent non-Hodgkin lymphoma with 131I-rituximab in routine clinical practice: 10-year single-institution experience of 142 consecutive patients. *Blood*, 117 (2011) 45.

9 Prasad V. The withdrawal of drugs for commercial reasons: the incomplete story of tositumomab. *JAMA Intern Med*, 174 (2014) 1887.

10 Chow VA, Rajendran JG, Fisher DR, Appelbaum FR, Cassaday RD, Martin PS, Holmberg LA, Gooley TA, Stevenson PA, Pagel JM & Green DJ, A phase II trial evaluating the efficacy of high-dose Radioiodinated Tositumomab (Anti-CD20) antibody, etoposide and cyclophosphamide followed by autologous transplantation, for high-risk relapsed or refractory non-hodgkin lymphoma. *Am J Hematol*, 95 (2020) 775.

11 Press OW, Unger JM, Rimsza LM, Friedberg JW, LeBlanc M, Czuczman MS, Kaminski M, Braziel RM, Spier C, Gopal AK & Maloney DG. Phase III randomized intergroup trial of CHOP plus rituximab compared with CHOP chemotherapy plus 131iodine-tositumomab for previously untreated follicular non-Hodgkin lymphoma: SWOG S0016. *J Clin Oncol*, 31 (2013) 314.

12 Kim EH, Ko HY, Yu AR, Kim H, Zaheer J, Kang HJ, Lim YC, Cho KD, Joo HY, Kang MK & Lee JJ. Inhibition of HIF-1α by Atorvastatin During 131I-RTX Therapy in Burkitt's Lymphoma Model. *Cancers*, 12 (2020) 1203.

13 Suman SK, Kameswaran M, Mallia M, Mittal S & Dash A. Synthesis and preliminary evaluation of 99mTc-Hynic-fragments [F(ab')$_2$ and F(ab')] of Rituximab as radioimmunoscintigraphic agents for patients with Non-Hodgkin's lymphoma. Appl Radiat and Isot, 153 (2019) 108808.

14 Lane DM, Eagle KF, Begent RH, Hope-Stone LD, Green AJ, Casey JL, Keep PA, Kelly AM, Ledermann JA & Glaser MG, Radioimmunotherapy of metastatic colorectal tumours with iodine-131-labelled antibody to carcinoembryonic antigen: phase I/II study with comparative biodistribution of intact and F (ab')$_2$ antibodies. *Br J Cancer*, 70 (1994) 521.

15 Vrigneaud JM, Dumont L, Vandroux D, Denat F, Cochet A, Brunotte F & Collin B, Radiolabeled F(ab′)2-cetuximab for theranostic purposes in colorectal and skin tumor-bearing mice models. *Clin Transl Oncol*, 17 (2018) 1.

16 Burvenich IJ, Schoonooghe S, Blanckaert P, Bacher K, Vervoort L, Coene E, Mertens N, De Vos F &Slegers G, Biodistribution and planar gamma camera imaging of ^{123}I- and ^{131}I-labeled F (ab′)$_2$ and Fab fragments of monoclonal antibody 14C5 in nude mice bearing an A549 lung tumor. *Nucl Med Biol*, 34 (2007) 257.

17 Wong KJ, Baidoo KE, Nayak TK, Garmestani K, Brechbiel MW & Milenic DE, *In vitro* and *in vivo* pre-clinical analysis of a F(ab')$_2$ fragment of panitumumab for molecular imaging and therapy of HER1-positive cancers. *EJNMMI Res*, 1 (2011) 1.

18 Rogers GT, Harwood PJ, Pedley RB, Boden J & Bagshawe KD, Dose-dependent localisation and potential for therapy of F (ab')$_2$ fragments against CEA studied in a human tumour xenograft model. *Br J Cancer*, 54 (1986) 341.

19 Pedley RB, Boden JA, Boden R, Dale R & Begent RH, Comparative radioimmunotherapy using intact or F (ab')$_2$ fragments of ^{131}I anti-CEA antibody in a colonic xenograft model. *Br J Cancer*, 68 (1993) 69.

20 Bäck T, Chouin N, Lindegren S, Kahu H, Jensen H, Albertsson P & Palm S, Cure of human ovarian carcinoma solid xenografts by fractionated α-radioimmunotherapy with 211At-MX35-F(ab′)$_2$: influence of absorbed tumor dose and effect on long-term survival. *J Nucl Med*, 58 (2017) 598.

21 Li L, Xu HY, Mi L, Bian HJ, Qin J, Xiong H, Feng Q, Wen N, Tian R, Xu LQ & Shen XM, Radioimmunotherapy of human colon cancer xenografts by using ^{131}I-labeled-CAb1 F(ab′)$_2$. *Int J Radiat Oncol Biol Phys*, 66 (2006) 1238.

22 Rao AV, Akabani G & Rizzieri DA, Radioimmunotherapy for non-Hodgkin's lymphoma. *Clin Med Res*, 3 (2005) 157.

23 Press OW & Rasey J, Principles of radioimmunotherapy for hematologists and oncologists. *Semin Oncol*, 27 (2000) 62.

24 Kameswaran M, Vimalnath KV, Rajeswari A, Joshi PV, Sarma HD & Samuel G. Clinical scale preparation and evaluation of ^{131}I-Rituximab for Non-Hodgkin's Lymphoma. *Radiochim Acta*, 102 (2014) 553.

25 Bhattacharya A, Venkataramarao SH, Bal CS & Mittal BR. Utility of Iodine-131 hybrid SPECT-CT fusion imaging before high-dose radioiodine therapy in papillary thyroid carcinoma. *Indian J Nucl Med*, 25 (2010) 29.

26 Wei L, Luo RC, Zhang JY, Yan X & Lü CW, *In vitro* cytotoxicity of ^{131}I-Rituximab against B-cell lymphoma cells. *Nan Fang Yi Ke Da Xue Xue Bao*, 29 (2009) 40.

27 Kumar C, Pandey BN, Samuel G & Venkatesh M, Cellular internalization and mechanism of cytotoxicity of 131I-rituximab in Raji cells. *J Environ Pathol Toxicol Oncol*, 32 (2013) 91.

28 Ambade RN, Shinde SN, Khan MS, Lohar SP, Vimalnath KV, Joshi PV, Chakraborty S, Pillai MR & Dash A, Development of a dry distillation technology for the production of 131I using medium flux reactor for radiopharmaceutical applications. *J Radioanal Nucl Chem*, 303 (2015) 451.

29 Laemmli UK, Cleavage of structural proteins during the assembly of the head of bacteriophage T4. *Nature*, 227 (1970) 680.

30 Hunter WM & Greenwood FC, Preparation of iodine-131 labeled growth hormone of high specific activity. *Nature*, 194 (1962) 495.

31 Mosmann T, Rapid colorimetric assay for cellular growth and survival: application to proliferation and cytotoxicity assays. *J Immunol Methods*, 65 (1983) 63.

32 Lobo ED, Hansen RJ & Balthasar JP. Antibody pharmacokinetics and pharmacodynamics. *J Pharm Sci*, 93 (2004) 2645.

33 Moldofsky PJ, Powe J, Mulhern Jr CB, Hammond N, Sears HF, Gatenby RA, Steplewski Z & Koprowski H, Metastatic colon carcinoma detected with radiolabeled F(ab')$_2$ monoclonal antibody fragments. *Radiology*, 149 (1983) 549.

34 Wahl RL, Parker CW & Philpott GW, Improved radioimaging and tumor localization with monoclonal F(ab')$_2$. *J Nucl Med*, 24 (1983) 316.

35 Riva P, Tison V, Arista A, Sturiale C, Franceschi G, Riva N, Casi M, Moscatelli G, Campori F & Spinelli A, Radioimmunotherapy of gastrointestinal cancer and glioblastomas. *Int J Biol Markers*, 8 (1993) 192

36 Wei L, Luo RC, Zhang JY, Yan X, Fang YX & Fei LH, Biological response of B-cell lymphoma cells *in vitro* to ^{131}I-rituximab. *Nan Fang Yi Ke Da Xue Xue Bao*, 26 (2006) 211.